

In Situ Positron Annihilation Spectroscopy Analysis on Low-Temperature Irradiated Semiconductors, Challenges and Possibilities

Jonatan Slotte,* Simo Kilpeläinen, Natalie Segercrantz, Kenichiro Mizohata, Jyrki Räisänen, and Filip Tuomisto

A unique experimental setup at the Accelerator Laboratory of the University of Helsinki enables in situ positron annihilation spectroscopy (PAS) analysis on ion irradiated samples. In addition, the system enables temperature control (10–300 K) of the sample both during irradiation and during subsequent positron annihilation measurements. Using such a system for defect identification and annealing studies comes with a plethora of possibilities for elaborate studies. However, the system also poses some restrictions and challenges to these possibilities, both related to irradiation and to the PAS analysis. This review tries to address these issues.

1. Introduction

Irradiation with electrons or light ions combined with a suitable technique to analyze irradiation damage is a commonly used technique to study irradiation damage and point defects in crystalline samples.^[1] A further improvement to such a study is temperature control of the irradiated sample combined with in situ characterization of the irradiation damage. Performing such experiments can be nontrivial, although the irradiation and temperature control of the sample is a fairly easy task. Difficulties can arise in the characterization process, if and when the characterization technique has restrictions on measurement conditions.

A simple extension of temperature-controlled irradiations of semiconductor samples, is to use ion beam analysis (IBA) for the damage study, i.e., utilize the same ion beam used for

irradiation or a beam generated with the same ion accelerator as a characterization tool.^[2] Although such an experiment performed with, e.g., Rutherford backscattering spectrometry in combination with ion channeling is useful for damage analysis,^[2] IBA does not allow for point defect analysis. Historically, the electron paramagnetic resonance (EPR) has been very successful in identifying point defects in irradiated silicon.^[3–5] More recently also deep level transient spectroscopy (DLTS) has been utilized on low-temperature irradiated samples.^[6] The challenge with DLTS is that the


technique itself is based on studying how charge carriers are trapped and released by defects with levels in the bandgap of semiconductors. These processes are studied as a function of temperature to identify the levels.^[7] Hence, elaborate annealing experiments at low temperatures cannot be performed.

Positron annihilation spectroscopy (PAS) is a renowned technique for defect characterization in semiconductors, especially suitable for vacancy defects. In addition to being defect sensitive, with the possibility to identify vacancy defects (chemical surrounding and size), a further advantage is the insensitivity to measurement conditions.^[8,9] This has enabled PAS to be utilized in defect studies in semiconductors in combination with, e.g., sample illumination for changing charge states of defects^[10–12] or by observing charge state transitions by moving the Fermi level thermally.^[13,14] An advantage of PAS is the sensitivity range of the spectroscopy, which coincides with typical doping levels in bulk semiconductor wafers, 10^{15} – 10^{18} cm⁻³. Furthermore, there has been a few studies where PAS has been used for low-temperature irradiation with subsequent annealing experiments. Hansen et al.^[15] used positron lifetime experiments to study hydrogen-defect interactions in molybdenum. In this study, the irradiations were performed with 6 MeV protons at 20 K with subsequent in situ PAS measurements. Mason and Coleman^[16] constructed an in situ implantation setup that enabled PAS Doppler broadening spectroscopy measurements with a variable energy positron beam on low-temperature implanted samples. This setup was later used for studying vacancy and interstitial migration in silicon implanted with 20 keV helium ions.^[17] Kinomura et al. used a similar setup to study ion implanted Fe and Ni in the temperature range 100–773 K.^[18]

A unique facility at the Accelerator Laboratory of the University of Helsinki was constructed in 2006.^[19] In this

Dr. J. Slotte, Dr. S. Kilpeläinen, Dr. N. Segercrantz, Prof. F. Tuomisto
Department of Applied Physics
Aalto University
P.O. 15100, FI-15100 Aalto, Finland
E-mail: jonatan.slotte@aalto.fi

Dr. J. Slotte, Dr. K. Mizohata, Prof. J. Räisänen, Prof. F. Tuomisto
Department of Physics
University of Helsinki
P.O. Box 43, FI-00014 Helsinki, Finland

 The ORCID identification number(s) for the author(s) of this article can be found under <https://doi.org/10.1002/pssa.202000232>.

© 2020 The Authors. Published by Wiley-VCH GmbH. This is an open access article under the terms of the Creative Commons Attribution-NonCommercial-NoDerivs License, which permits use and distribution in any medium, provided the original work is properly cited, the use is non-commercial and no modifications or adaptations are made.

DOI: 10.1002/pssa.202000232

experimental setup, a positron lifetime measurement apparatus is constructed around the beam line of a 5 MV tandem accelerator. This setup makes it possible to perform positron lifetime measurements in situ on proton irradiated samples in the temperature range 10–300 K with proton energies up to 10 MeV. A few studies have so far been conducted with this equipment.^[20,21] In this review, we address the challenges that one has to overcome to successfully utilize the PAS technique on low-temperature irradiated samples as well as how to explore the possibilities PAS can offer for point-defect identification in semiconductors.

2. Experimental Setup

A detailed description of the experimental setup can be found in ref. [19]. A traditional sandwich sample package is used for the PAS measurements, see **Figure 1**. The ²²Na source, consisting of radioactive NaCl, is encapsulated in a thin Al-foil, thickness 2 μm, and surrounded on both sides by two identical samples. The sample package is mounted on a copper sample holder, with a circular aperture (≈80 mm²) for the ion beam. The sample holder is in thermal contact with a closed-cycle helium cryostat and can be shifted mechanically between two positions. In the lower position, the sample is irradiated, and in the higher position, the PAS measurements are performed. Hence, PAS measurements during irradiation is not possible. A conventional fast–fast coincidence system with plastic scintillators and a time resolution of 260 ps is used for the PAS measurements.

For successful irradiation experiments, it is essential to be able to measure the ion beam fluence to a high accuracy. This is ensured in this setup by lowering the sample and driving the ion beam into a Faraday cup, with which the absolute ion current is measured. This result is then used for calibrating a beam profilometer placed in front of the sample under irradiation. Typically, the ion flux in an irradiation with this setup

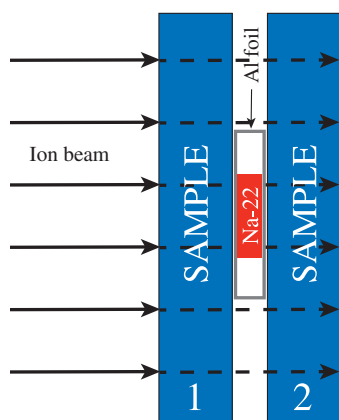


Figure 1. Schematic figure of the sample sandwich package during irradiation. The beamline is in the plane of the figure from left to right. The different parts of the sample package are not plotted in scale. The thickness of the source and the Al foil wrapping is <5 μm. As only around 3% of the positron annihilate within source and the wrapping, possible damage in source and the Al foil need not be considered. The samples are typically 400–500 μm thick.

is of the order of 10¹⁵ cm⁻² h⁻¹ for 9 MeV protons, enabling irradiation fluences up to 10¹⁶ cm⁻² with reasonable irradiation times.

3. Experimental Planning

3.1. Proton Irradiation

For defect studies in crystalline material where the defects are produced by bombarding the sample with charged particles, the defect distribution will depend on the host lattice, the mass of the charged particle, and on its incident energy. In annealing studies, where the goal is to investigate the annealing energetics and kinetics of a particular point defect, a homogenous defect distribution is usually desired. This requires that the sensitivity depth of the used defect spectroscopy tool is within the track region of the irradiation particle, i.e., the deposited energy is more or less constant as a function of depth. This requirement restricts how sample material, irradiation energy, and different spectroscopies can be combined.

Traditionally, electron irradiation in the energy range 1–3 MeV has been used for producing homogenous defect distributions, e.g., DLTS,^[6] PAS,^[22–25] and EPR.^[4] Although electron irradiation is a good tool for such studies, there are some drawbacks especially from a PAS perspective. For example, the irradiation currents are typically quite low. Hence, the irradiation times tend to be quite long to produce enough defects to get over the PAS sensitivity limit.

Ion irradiation, especially proton irradiation, is therefore a viable option for defect production in samples for PAS studies. In a point defect study, the desire is that the studied depth interval of the sample is within the track region of the irradiation particle. Here, the deposited energy is fairly homogenous and consequently also the damage production. This requirement can be a challenge for in situ defect studies with PAS. As can be seen from the ion distributions for a 10 MeV proton irradiation in **Figure 2**, the ion range in Si is roughly at a depth 200–300 μm in sample 2 of the sample package. This is deep enough to avoid a significant influence from end-of-range defects in Si, where the mean positron penetration depth from the used

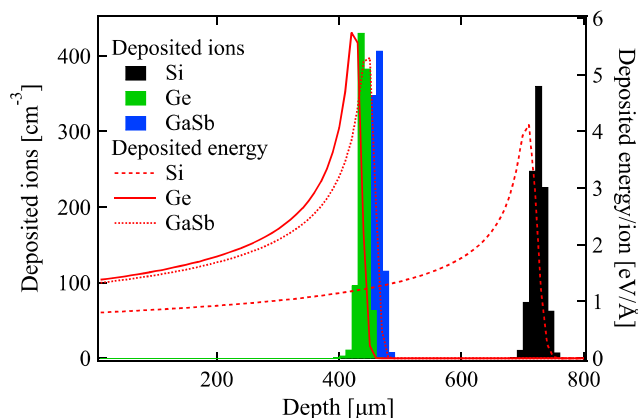


Figure 2. Stopping and Range of Ions in Matter^[26] simulation of 10 MeV proton irradiation into Si, Ge, and GaSb. The histograms depict deposited ions (left axis) and the lines deposited energy (right axis).

e^+ -source ^{22}Na is around $50\ \mu\text{m}$.^[27] However, as is evident from Figure 2, the ion range will be a problem especially in semiconductors with densities of $\approx 5\ \text{g cm}^{-3}$ and above. The ion range in denser semiconductors is below $500\ \mu\text{m}$, which results in end-of-range defects dominating the PAS results if the sample thickness is $400\text{--}500\ \mu\text{m}$.

3.2. PAS Measurements

To study a homogenous defect distribution, the end of range in sample 2 has to be shifted deeper into the sample. This can be done in two ways, either by increasing the ion range, i.e., increasing the energy of the irradiation ion or by reducing the track length in sample 1. Even if an increase in irradiation energy could be achieved, this is not necessarily a good approach, as already a $10\ \text{MeV}$ proton beam can activate the samples to some extent. Increasing the proton energy will further activate the sample.

In our previous studies,^[20,21] the end of range of the ions was shifted deeper into sample 2 by mechanically grinding sample 1 thinner. A few things need to be considered when performing the thinning. Irrespective of the method used, defects due to the thinning process can influence the PAS measurements. Hence, it is of utmost importance that the pristine surface of sample 1 faces the e^+ -source. Furthermore, sample 1 cannot be made arbitrarily thin, as one has to also consider the e^+ implantation depth. The thinning of sample 1 will also make it more brittle and caution need to be taken when the sample package is mounted to the sample holder, as cracks in the sample will influence the PAS measurements. For the Ge ^[20] and GaSb ^[21] studies, where the density of the sample material is above $5\ \text{g cm}^{-3}$, sample 1 was thinned to a thickness of $\approx 250\ \mu\text{m}$. This allowed for enough thickness in sample 1 to ensure that the amount of positrons reaching the sample surface was insignificant. Consequently, the end of range of the ions in sample 2 was shifted below $150\ \mu\text{m}$.

As mentioned earlier, sample activation is also something that has to be considered. This applies especially to semiconductors and compound semiconductors consisting of heavier nuclei, e.g., from the fourth row of the periodic table Ga, Ge, and As or heavier such as In and Sb. Irrespective of the primary nuclear reaction, most activated isotopes emit γ -rays that can be detected by the scintillators used in the PAS measurements. This will cause unwanted background in the positron lifetime and Doppler broadening spectra. However, only if the half life of the activated isotope is of the same order of magnitude as the measurement time of the PAS experiment, measures have to be taken. Isotopes with (very) short lifetimes, $< 100\ \text{s}$, will decay before they can influence the PAS experiments. If the decay times of the isotopes are months or longer, the activity of such isotopes is too small to have any significant impact on the PAS measurements.

An e^+ -source, used for regular lifetime measurements, has an activity of the order of $1\ \text{MBq}$, which translates into a measurement time for a typical lifetime spectrum with 10^6 counts of roughly $1\ \text{h}$. For an annealing series, $5\text{--}20$ such spectra are collected. This means that a measurement takes from a few hours to ≈ 2 days. Hence, if the irradiation causes a significant activation of an isotope with a half life from a few hours to a few days, this isotope has to be let to decay enough before the measurement is

started. If the irradiation is done at low temperatures, the sample has to be kept cool during this time.

4. Examples

4.1. The Monovacancy in Ge

The aim of this study^[20] was to identify the monovacancy in Ge and to study its annealing behavior. No measurements with a spectroscopy able to unambiguously identify a point defect, such as EPR, had previously been made on the monovacancy in Ge. However indirect evidence on migration^[28–30] and formation energies,^[31–37] and on the annealing of the Frenkel pair^[6,38,39] had been obtained.

To identify a native point defect, such as the monovacancy, in a Ge with PAS, the sample cannot contain any impurities or dopants at concentrations of the same order of magnitude or higher as the expected point-defect concentration. Furthermore, the irradiation fluence should be chosen so that the measured spectrum can be decomposed into components, i.e., two lifetime components can be deduced from the spectrum: 1) the defect-specific lifetime (typically denoted as τ_2) and 2) the reduced bulk lifetime (typically denoted as τ_1).^[27] This means that the concentration of the studied point defect should be lower than the lower limit of saturation trapping to that defect. As a rule of thumb, this means that the concentration of a monovacancy-size defect should be in the $10^{17}\text{--}10^{18}\ \text{cm}^{-3}$ range. Typically, the lifetime of a positron in a monovacancy-size defect is $15\text{--}20\%$ above the lifetime of a defect-free bulk sample in traditional semiconductors (Si, Ge) or in compound semiconductors where the sizes of the atoms are similar (e.g., GaAs). Without prior knowledge on the positron lifetime in a monovacancy in Ge, with a bulk lifetime of $\approx 230\ \text{ps}$, the average positron lifetime should be in the $240\text{--}260\ \text{ps}$ range in the as-irradiated sample, see Figure 3. The average positron lifetime is a trapping model^[40] independent parameter, which can be deduced as the center of mass of the measured lifetime spectrum.

After tuning the irradiation fluence to the aforementioned level, the results shown in Figure 3a were measured after irradiation at $35\ \text{K}$. It should be noted that all PAS lifetime measurements of Figure 3 were performed at $35\ \text{K}$, i.e., no annealing occurred during the collection of the lifetime spectra. The annealings were performed in $30\ \text{min}$ steps at each annealing temperature and two annealing stages were observed, one at $100\ \text{K}$ and a second at $200\ \text{K}$, Figure 3a. Despite a successful annealing experiment, the lifetime spectra could not be fitted reliably with a two-trap trapping model below $200\ \text{K}$. An easy check point to see whether the trapping model gives reliable results, is the behavior of the reduced bulk lifetime

$$\tau_1 = \frac{1}{\lambda_b + \kappa_D} \quad (1)$$

where $\lambda_b = \tau_b^{-1}$ is the bulk annihilation rate and κ_D is the defect trapping rate. Hence, if the trapping model fit to the lifetime spectrum yields a τ_1 with a value similar or larger than the bulk lifetime ($\tau_b = 230\ \text{ps}$ in Ge), the two-trap model is void and a third lifetime component is being mixed into τ_1 . As shown in Figure 4, τ_1 is clearly too high below $100\ \text{K}$, rendering these points unphysical. From 100 to $200\ \text{K}$, during the first annealing

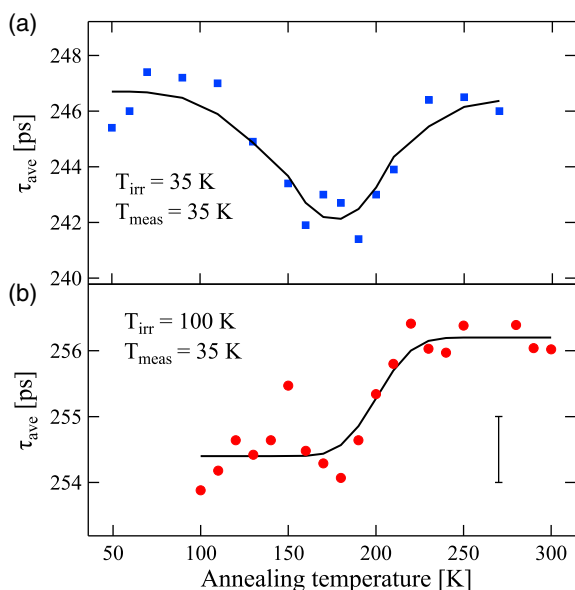


Figure 3. Average positron lifetime as a function of annealing temperature in 9–10 MeV proton irradiated Ge. The data from ref. [20]. The results in panel (a) were measured after irradiation at 35 K and the results in panel (b) after irradiation at 100 K. The fluence was $(1\text{--}3) \times 10^{14} \text{ cm}^{-2}$. The error in the average lifetime, $\Delta\tau_{\text{ave}} = \pm 0.5 \text{ ps}$ is indicated in the panel (b).

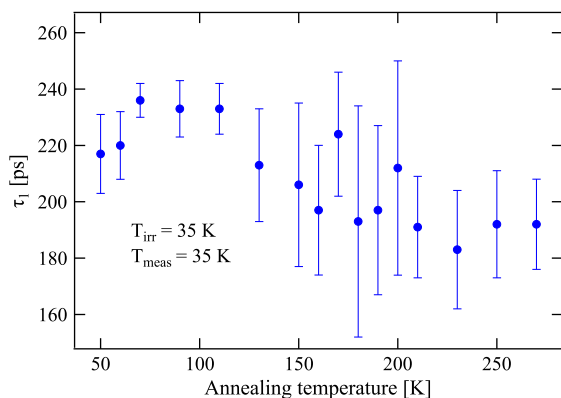


Figure 4. Two-trap model fit results for τ_1 for the sample irradiated at 35 K, Figure 3a. The data from ref. [20].

stage, the results are inconclusive due to the large errors in the fit. Above 200 K, τ_1 behaves according to the two-trap model. A consequence of the results in Figure 4 was that no conclusions on the nature of the first annealing stage could be drawn.

From previous DLTS studies, a level associated with the Frenkel pair in $\text{Ge}^{[6]}$ was found to anneal at 65 K. This fits fairly well with the first annealing stage in Figure 3a. To study the annealing of the isolated vacancy in Ge, this first annealing stage has to be avoided. With the experimental setup at the University of Helsinki and with insensitivity to measurement conditions of PAS, this is a fairly easy task. Hence, a second sample was irradiated at 100 K, cooled to 35 K after irradiation and kept at 35 K for ≈ 4 days (to avoid unwanted background from activated isotopes). The annealing series for this sample is shown in

Figure 3b. As expected the first annealing stage is absent and the lifetime spectra could be decomposed successfully into two components. A defect-specific lifetime component for the monovacancy in germanium of $272 \pm 4 \text{ ps}$ was obtained.

4.2. The Instability of the Sb Vacancy in GaSb

The compound semiconductor GaSb has a peculiar feature compared with other III–V semiconductors, such as GaAs: The self diffusivity on the two sublattices differ by several orders of magnitude. Bracht et al. suggested that the reason behind this behavior is the instability of the Sb vacancy,^[41] i.e., the reaction



occurs at a very low temperature. Hence, there are almost no Sb vacancies available to mediate diffusion on the Sb sublattice. A further consequence of the instability of the Sb vacancy is the abundant creation of Ga antisites that play an important role in the p-type conductivity of as-grown bulk GaSb.^[42] Also from a PAS point of view, GaSb has some interesting properties. Ling et al. reported that the main culprit responsible for the p-type conductivity in undoped Czochralski-grown was not of vacancy nature.^[43] These findings were later confirmed by Kujala et al., who found that the negatively charged Ga antisite was one of the two dominating positron traps at room temperature, together with the Ga vacancy.^[42]

To study the instability of the Sb vacancy in GaSb and the onset of the reaction (2), we performed carefully designed irradiation experiments with subsequent ex situ and in situ PAS analysis on Czochralski-grown undoped and p-type bulk GaSb.^[21] In addition to the challenges mentioned in the previous sections concerning Ge, i.e., proton range and isotope activation, further challenges had to be overcome for a successful outcome of the study. First, both the undoped and p-type GaSb contain a significant amount of positron traps, V_{Ga} and Ga_{Sb} . Second, as GaSb is a compound semiconductor, vacancies will be created on both sublattices. Hence, the PAS measurements will be dominated by the as-grown defects up to a certain irradiation fluence. Furthermore, the dominating defects in the as-grown material are related to the reaction (2), i.e., V_{Ga} and Ga_{Sb} . Luckily, the production rates for defects on the two sublattices differ in favor of Sb vacancies by roughly 40%.^[21,44]

Figure 5 shows the results for two low-temperature irradiated samples. Prior to the low-temperature irradiation, ex situ irradiations had been performed to tune the fluence to an appropriate level. As the as-grown samples already contain two competing positron traps and the low-temperature irradiated samples also contain V_{Sb} , no decomposition of the lifetime spectra was possible at any point of the annealing series. As shown in Figure 5a, clear annealing step in the average positron lifetime is observed for the sample irradiated with higher fluence. This step was attributed to the annealing of V_{Sb} . For the sample irradiated with a lower fluence, no such step is observed, as the irradiation fluence is not high enough to create enough V_{Sb} compared with the as-grown defects V_{Ga} and Ga_{Sb} . An energy barrier for the reaction (2) of $0.6 \pm 0.1 \text{ eV}$ was obtained by fitting an annealing model to the average positron lifetime. For details on the annealing model, see ref. [21].

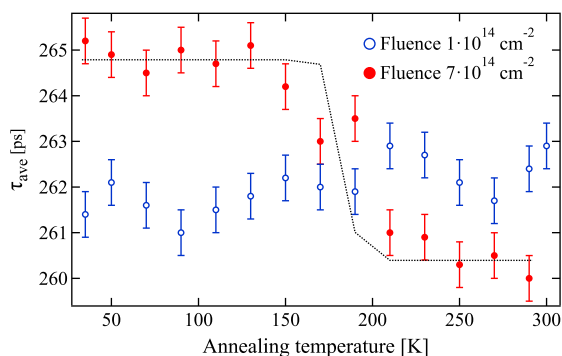


Figure 5. Average positron lifetime as a function of annealing temperature. The irradiation and measurement temperature was 35 K and the annealing time per step was 30 min. The dotted line is a fit of an annealing model according to reaction (2). The average lifetime of the as-grown p-type GaSb sample was 257 ps at 35 K. Data from ref. [21].

5. Conclusion

The scope of this review has been to show how the versatility of the PAS technique can be utilized for studying point defects in low-temperature irradiated semiconductors. Although the technique itself is versatile, performing such experiments has its challenges and some precautions have to be taken to ensure a successful experiment. In no particular order, these precautions include at least: 1) Choosing the irradiation fluence carefully. 2) Ensuring that the positrons mainly probe a homogenous defects distribution in the track region of the ions. 3) Be aware of possible activation of the irradiated samples and take precautions to avoid any significant influence of decaying activated isotopes on the PAS measurements. All of these points relate both to the PAS technique and to the irradiation process itself. Although the examples presented in this review concern proton irradiation, similar experiments can also be performed with the present equipment on samples irradiated or implanted with heavier ions.

Conflict of Interest

The authors declare no conflict of interest.

Keywords

defects, irradiation, positron annihilation spectroscopy, vacancies

Received: April 18, 2020

Revised: June 9, 2020

Published online: August 2, 2020

- [1] K. Nordlund, S. J. Zinkle, A. E. Sand, F. Granberg, R. S. Averback, R. E. Stoller, T. Suzudo, L. Malerba, F. Banhart, W. J. Weber, F. Willaime, S. L. Dudarev, D. Simeone, *J. Nucl. Mat.* **2018**, 512, 450.
- [2] C. Jaynes, R. P. Webb, *Rev. Accl. Sci. Tech.* **2011**, 4, 41.
- [3] G. Watkins, *Deep Centers in Semiconductors* (Ed: T. Pantelides), Gordon Breach, New York **1986**.
- [4] G. D. Watkins, J. W. Corbett, *Phys. Rev.* **1964**, 134, A1359.

- [5] G. D. Watkins, *IEEE Trans. Nucl. Sci.* **1969**, NS-16, 13.
- [6] A. Mesli, L. Dobaczewski, K. B. Nielsen, V. Kolkovsky, M. C. Petersen, A. Nylandsted Larsen, *Phys. Rev. B* **2008**, 78, 165202.
- [7] D. V. Lang, *J. Appl. Phys.* **1974**, 45, 3023.
- [8] F. Tuomisto, I. Makkonen, *Rev. Mod. Phys.* **2013**, 85, 1584.
- [9] J. Slotte, I. Makkonen, F. Tuomisto, *Characterisation and Control of Defects in Semiconductors* (Ed: F. Tuomisto), IET, London **2020**.
- [10] R. Krause, K. Saarinen, P. Hautojärvi, A. Polity, G. Gärtner, C. Corbel, *Phys. Rev. Lett.* **1990**, 65, 3329.
- [11] S. Arpiainen, K. Saarinen, P. Hautojärvi, L. Henry, M. F. Barthe, C. Corbel, *Phys. Rev. B* **2002**, 66, 075206.
- [12] J. M. Mäki, F. Tuomisto, A. Varpula, D. Fisher, R. U. A. Khan, P. M. Martineau, *Phys. Rev. Lett.* **2011**, 107, 217403.
- [13] K. Kuitunen, F. Tuomisto, J. Slotte, *Phys. Rev. B* **2007**, 76, 233202.
- [14] J. Slotte, K. Saarinen, A. Salmi, S. Simula, R. Aavikko, P. Hautojärvi, *Phys. Rev. B* **2003**, 67, 115209.
- [15] H. E. Hansen, R. Talja, H. Rajainmäki, H. K. Nielsen, B. Nielsen, R. M. Nieminen, *Appl. Phys. A* **1985**, 36, 81.
- [16] R. E. Mason, P. G. Coleman, *Appl. Surf. Sci.* **2006**, 252, 3228.
- [17] P. G. Coleman, C. P. Burrows, *Phys. Rev. Lett.* **2007**, 98, 265502.
- [18] A. Kinomura, R. Suzuki, T. Ohdaira, K. Ito, Y. Kobayashi, T. Iwai, *J. Phys.: Conf. Series* **2011**, 262, 012029.
- [19] S. Väyrynen, P. Pusa, P. Sane, P. Tikkanen, J. Räisänen, K. Kuitunen, F. Tuomisto, J. Härkönen, I. Kassamakov, E. Tuominen, E. Tuovinen, *Nucl. Instr. Methods A* **2007**, 572, 978.
- [20] J. Slotte, S. Kilpeläinen, F. Tuomisto, J. Räisänen, A. Nylandsted Larsen, *Phys. Rev. B* **2011**, 83, 235212.
- [21] N. Segercrantz, J. Slotte, F. Tuomisto, K. Mizohata, J. Räisänen, *Phys. Rev. B* **2017**, 95, 184103.
- [22] C. Corbel, P. Hautojävi, M. Stucky, *Ann. Chim. Fr.* **1985**, 10, 733.
- [23] A. Polity, F. Rudolf, *Phys. Rev. B* **1999**, 59, 10025.
- [24] V. Ranki, A. Pelli, K. Saarinen, *Phys. Rev. B* **2004**, 69, 115205.
- [25] K. E. Knutsen, A. Galeckas, A. Zubiaga, F. Tuomisto, G. C. Farlow, B. G. Svensson, A. Y. Kuznetsov, *Phys. Rev. B* **2012**, 86, 121203.
- [26] J. F. Ziegler, M. D. Ziegler, J. P. Biersack, *Nucl. Instr. Methods B* **2010**, 268, 1818.
- [27] R. Krause-Rehberg, H. S. Leipner, *Positron Annihilation in Semiconductors*, Springer, Berlin **1999**.
- [28] R. E. Whan, *Phys. Rev.* **1965**, 140, 690.
- [29] S. N. Ershov, V. A. Pantaleev, S. N. Nagornkh, V. V. Chernyakhovskii, *Sov. Phys. Solid State* **1977**, 19, 187.
- [30] D. Shaw, *Phys. Status Solidi B* **1975**, 72, 11.
- [31] A. Giese, N. A. Stolwijk, H. Bracht, *Appl. Phys. Lett.* **2000**, 77, 642.
- [32] S. Mayburg, *Phys. Rev.* **1954**, 95, 38.
- [33] R. A. Logan, *Phys. Rev.* **1956**, 101, 1455.
- [34] A. G. Tweet, *Phys. Rev.* **1957**, 106, 221.
- [35] A. G. Tweet, *J. Appl. Phys.* **1959**, 30, 2002.
- [36] A. Hiraki, Y. Suita, *Technol. Rep. Osaka Univ.* **1965**, 15, 65.
- [37] L. F. Konorova, *Sov. Phys. Solid State* **1969**, 10, 2233.
- [38] V. Ermtsev, *Mater. Sci. Semicond. Process* **2006**, 9, 580.
- [39] T. A. Callcott, J. W. Machay, *Phys. Rev.* **1967**, 161, 698.
- [40] R. N. West, *Positrons in Solids* (Ed: P. Hautojärvi), Springer Verlag, Heidelberg **1979**.
- [41] H. Bracht, S. P. Nicols, J. P. S. W. Walukiewicz, F. Briones, E. Haller, *Nature* **2000**, 408, 69.
- [42] J. Kujala, N. Segercrantz, F. Tuomisto, J. Slotte, *J. Appl. Phys.* **2014**, 116, 143508.
- [43] C. C. Ling, M. K. Lui, S. K. Ma, X. D. Chen, S. Fung, C. D. Beling, *Appl. Phys. Lett.* **2004**, 85, 384.
- [44] F. Agulló-López, C. R. A. Catlow, P. D. Townsend, *Point Defects in Materials*, Academic Press, New York **1988**.



Jonatan Slotte received his Ph.D. in physics from the University of Helsinki in 1999. His thesis was related to diffusion of impurities and vacancies in semiconductors. For the last 20 years his research has been focused on point defects in semiconductors, and the main experimental tool he uses is positron annihilation spectroscopy.



Filip Tuomisto studied engineering physics and mathematics at the Helsinki University of Technology (M.Sc. and D.Sc.). He is now a professor of experimental materials physics at University of Helsinki where he is head of the Accelerator Laboratory. His research focuses on the physics of point defects in semiconductors and metals.



Jyrki Räisänen is a professor of physics and head of the Department of Physics at Helsinki University. He received his Ph.D. in 1981 from the University of Helsinki. His research interests are ion beam interactions and applications.